Effects of the temperature and magnetic-field dependent coupling on the properties of QCD matter

Li Yang and Xin-Jian Wen[*]

Institute of Theoretical Physics, Shanxi University, Taiyuan 030006, China
(Received 10 April 2017; published 25 September 2017)

To reflect the asymptotic freedom in the thermal direction, a temperature-dependent coupling was proposed in the literature. We investigate its effect on QCD matter with and without strong magnetic fields. Compared with the fixed coupling constant, the running coupling leads to a drastic change in the dynamical quark mass, entropy density, sound velocity, and specific heat. The crossover transition of QCD matter at finite temperature is characterized by the pseudocritical temperature T_{pc}, which is generally determined by the peak of the derivative of the quark condensate with respect to the temperature $d\phi/dT$, or equivalently, by the derivative of the quark dynamical mass dM/dT. In a strong magnetic field, the temperature- and magnetic-field-dependent coupling $G(eB, T)$ was recently introduced to account for inverse magnetic catalysis. We propose an analytical relation between the two criteria $d\phi/dT$ and dM/dT and show a discrepancy between them in finding the pseudocritical temperature. The magnitude of the discrepancy depends on the behavior of dG/dT.

I. INTRODUCTION

It is well known that with increasing baryon number density and temperature, hadronic matter undergoes a phase transition to quark-gluon plasma. In high-temperature or high-density regions, asymptotic freedom becomes important in the investigation of the QCD diagram [1]. To obtain a comprehensive QCD diagram, it is necessary to understand the phase transition in the presence of magnetic fields. In recent years, research related to strong magnetic fields has been carried out in both condensed matter physics [2] and particle physics [3]. Strong magnetic fields could have a drastic influence on the special stability of quark matter [4–6], the anisotropy of the equation of state [7], the region of the phase transition, and (inverse) magnetic catalysis. The presence of magnetic fields can promote a change in the size and location of the first-order line [8] and increase the mass of neutron stars and white dwarf stars beyond the Chandrasekhar limit [9]. Both thermodynamical and dynamical quantities display an oscillating behavior in the presence of magnetic fields [10]. Magnetic catalysis was found to have an important effect on chiral symmetry breaking enhanced by an external magnetic field [11–14].

The Nambu–Jona-Lasinio (NJL) model has been successful in investigating the QCD diagram, and recently it was extended to easily reproduce the behavior of the quark condensate and the dynamical mass with an external magnetic field [15,16]. It was further extended by including tensor channels (which leads to a spin-one condensate [17]) or by including the eight-quark interaction [18]. In addition to the magnetic effect at vanishing chemical potential,

inverse magnetic catalysis was initially suggested as a mechanism to decrease the critical chemical potential for chiral restoration [19]. It was later predicted by lattice simulations at zero density that the critical temperature of the chiral transition decreases with the magnetic field [20]. It has also recently attracted much theoretical attention in various phenomenological models [21,22]. It is apparent that the failure of the previous effective models to provide inverse magnetic catalysis can be attributed to the fact that the coupling constant does not run with the magnetic field [23], or strictly speaking, the effective models lack gluonic degrees of freedom and cannot account for the backreaction of sea quarks to the magnetic field [24].

Many attempts have been made to interpret inverse magnetic catalysis. One approach is through a magnetic-field- and temperature-dependent coupling [23,24] or a parametrized fitting function [25] taking into account the asymptotic-freedom effect near the critical point. Another approach is through the parametrization of the Polyakov loop (whose coefficients depend on both the temperature and magnetic field) to mimic the reaction of the gluon sector to the magnetic field [26]. In fact, the employment of asymptotic freedom in the phenomenological approach can be traced to early works in the literature. For example, the QCD coupling was introduced to depend on the environmental parameters, such as the density [27], temperature [28], and magnetic field [13,25]. Based on the general argument from the renormalization group equation [29], these characteristics replace the momentum as the running scale. The special running behavior will lead to a detailed change in the properties of QCD matter. The magnetic-field-dependent running coupling reveals interesting properties, such as a change in the dynamical mass and the

_____
[*]wenxj@sxu.edu.cn

stability of magnetized quark matter [30–32]. One recent work reported that the magnetization changes due to the variation of the coupling constant with respect to the magnetic field $\partial G/\partial B$ [24]. Then, one may ask about the contribution of $\partial G/\partial T$. In this paper, we first analyze the behavior of the coupling dependent on the temperature in two-flavor quark matter. Then, we investigate the influence of the temperature- and magnetic-field-dependent coupling on the pseudocritical temperature of the crossover transition in a strong magnetic field.

This work is organized as follows. In Sec. II, we briefly review the NJL model of quark matter in both zero magnetic field and a strong magnetic field. Correspondingly, the two kinds of running couplings are introduced as well as the model parameters in the computation. In Sec. III, the numerical results and a discussion are given, with a detailed analysis of the effects of the running coupling on the thermodynamical quantities. The last section is a short summary.

II. THERMODYNAMICS OF THE SU(2) NJL MODEL

A. Thermodynamics of the SU(2) NJL Model in zero magnetic field

In the SU(2) version of the NJL model without a magnetic field, the Lagrangian density of the two-flavor NJL model is given by

$$\mathcal{L}_{NJL} = \bar{\psi}(i\slashed{\partial} - m)\psi + G[(\bar{\psi}\psi)^2 + (\bar{\psi}i\gamma_5\vec{\tau}\psi)^2], \quad (1)$$

where ψ represents a flavor isodoublet (u and d quarks) and $\vec{\tau}$ are isospin Pauli matrices. In the mean-field approximation [33], the dynamical quark mass is

$$M_i = m - 2G\langle\bar{\psi}\psi\rangle, \quad (2)$$

where the quark condensates include u and d quark contributions as $\langle\bar{\psi}\psi\rangle \equiv \phi = \sum_{i=u,d}\phi_i$. The dynamical mass depends on both flavor condensates. Therefore, the same mass $M_u = M_d = M$ is available for u and d quarks. The contribution from the quark with flavor i is

$$\phi_i = \phi_i^{vac} + \phi_i^{med}. \quad (3)$$

The terms ϕ_i^{vac} and ϕ_i^{med} represent the vacuum and medium contributions to the quark condensation, respectively,

$$\phi_i^{vac} = -\frac{MN_c}{2\pi^2}\left[\Lambda\sqrt{\Lambda^2 + M^2} - M^2\ln\left(\frac{\Lambda + \sqrt{\Lambda^2 + M^2}}{M}\right)\right], \quad (4)$$

$$\phi_i^{med} = \frac{2MN_c}{\pi^2}\int_0^\infty \frac{f}{E^*}p^2dp, \quad (5)$$

where the effective quantity is $E^* = \sqrt{p^2 + M^2}$, and the fermion distribution function is defined as

$$f = \frac{1}{1 + \exp[E^*/T]}. \quad (6)$$

The total thermodynamic potential density in the mean-field approximation reads

$$\Omega = \frac{(M - m_0)^2}{4G} + \sum_{i=u,d}\Omega_i, \quad (7)$$

where the first term is the interaction term. In the second term, Ω_i is defined as $\Omega_i = \Omega_i^{vac} + \Omega_i^{med}$. The vacuum and medium contributions to the thermodynamic potential are

$$\Omega_i^{vac} = \frac{N_c}{8\pi^2}\left[M^4\ln\left(\frac{\Lambda + \epsilon_\Lambda}{M}\right) - \epsilon_\Lambda\Lambda(\Lambda^2 + \epsilon_\Lambda^2)\right], \quad (8)$$

$$\Omega_i^{med} = -\frac{2TN_c}{\pi^2}\int_0^\infty\left\{\ln\left[1 + \exp\left(-\frac{E^*}{T}\right)\right]\right\}p^2dp, \quad (9)$$

where the quantity ϵ_Λ is defined as $\epsilon_\Lambda = \sqrt{\Lambda^2 + M^2}$. The ultraviolet divergence in the vacuum part Ω_i^{vac} of the thermodynamic potential is removed by the momentum cutoff. The effective pressure in the system is corrected by defining $P^{eff}(T) = P(T) - P(0)$. The sound velocity, specific heat, and entropy density from the flavor i contribution are given as [24,34]

$$c_s^2 = \frac{\partial P^{eff}}{\partial \epsilon}\bigg|_S, \qquad C_V = T\frac{\partial^2 P^{eff}}{\partial T^2}\bigg|_V, \quad (10)$$

$$S_i = -\frac{2N_c}{\pi^2}\int_0^\infty[f\ln(f) + (1 - f)\ln(1 - f)]p^2dp. \quad (11)$$

In principle, the interaction coupling constant between quarks should be solved by the renormalization group equation, or it can be phenomenologically expressed in an effective potential dependent on environmental variables [35–37]. In the infrared region, the nonperturbative effect becomes important and the dynamical gluon mass represents the confinement feature of QCD [38]. Here we adopt the temperature-dependent running coupling to investigate the thermal effect in the high-temperature region [1],

$$G'(T) = G_0\sqrt{1 - \left(\frac{T}{T_0}\right)^2}, \quad (12)$$

where $T_0 = 0.3\ \Lambda$ is the critical temperature.

B. Thermodynamics of the SU(2) NJL model in a strong magnetic field

In the presence of strong external magnetic fields, the Lagrangian density of the two-flavor NJL model in a strong magnetic field is given as

$$\mathcal{L}_{NJL} = \bar{\psi}(i\slashed{D} - m)\psi + G[(\bar{\psi}\psi)^2 + (\bar{\psi}i\gamma_5\vec{\tau}\psi)^2], \quad (13)$$

where the covariant derivative $D_\mu = \partial_\mu - iq_iA_\mu$ represents the coupling of the quarks to the electromagnetic field (a sum over flavor and color degrees of freedom is implicit). The dynamical quark mass is the same as Eq. (2), but the quark condensates should include an additional term from the magnetic field contribution,

$$\phi_i = \phi_i^{\text{vac}} + \phi_i^{\text{mag}} + \phi_i^{\text{med}}, \quad (14)$$

where the vacuum contribution ϕ_i^{vac} is the same as Eq. (4). The magnetic field and medium contributions to the quark condensation are [15,39]

$$\phi_i^{\text{mag}} = -\frac{M|q_i|BN_c}{2\pi^2}\left\{\ln[\Gamma(x_i)] - \frac{1}{2}\ln(2\pi) + x_i\right.$$
$$\left. - \frac{1}{2}(2x_i - 1)\ln(x_i)\right\}, \quad (15)$$

$$\phi_i^{\text{med}} = \sum_{k_i=0} a_{k_i}\frac{M|q_i|BN_c}{2\pi^2}\int \frac{f_i}{E_i^*}dp, \quad (16)$$

where $a_{k_i} = 2 - \delta_{k0}$ and k_i are the degeneracy label and the Landau quantum number, respectively. The dimensionless quantity x_i is defined as $x_i = M^2/(2|q_i|B)$. It can be seen that the quark condensation is greatly strengthened by the factor $|q_iB|$ together with the dimensional reduction $D - 2$ [13,40]. In the second equation above, the temperature contribution with zero chemical potential is introduced in the fermion distribution function as

$$f_i = \frac{1}{1 + \exp[E_i^*/T]}. \quad (17)$$

The effective quantity $E_i^* = \sqrt{p^2 + s_i^2}$ sensitively depends on the magnetic field through $s_i = \sqrt{M^2 + 2k_i|q_i|B}$.

Accordingly, the thermodynamic potential density Ω_i becomes a sum of three terms,

$$\Omega_i = \Omega_i^{\text{vac}} + \Omega_i^{\text{mag}} + \Omega_i^{\text{med}}, \quad (18)$$

where only the second and third terms feel the strong magnetic field and should be rewritten as

$$\Omega_i^{\text{mag}} = -\frac{N_c(|q_i|B)^2}{2\pi^2}\left[\zeta'(-1, x_i) - \frac{1}{2}(x_i^2 - x_i)\ln(x_i) + \frac{x_i^2}{4}\right], \quad (19)$$

$$\Omega_i^{\text{med}} = -T\sum_{k=0} a_{k_i}\frac{|q_i|BN_c}{2\pi^2}\int dp\left\{\ln\left[1 + \exp\left(-\frac{E_i^*}{T}\right)\right]\right\}, \quad (20)$$

where $\zeta(a, x) = \sum_{n=0}^{\infty}\frac{1}{(a+n)^x}$ is the Hurwitz zeta function.

In the presence of a strong magnetic field, it is well known that the interaction constant shows an obvious decreasing behavior in addition to the enlargement of the gluon mass [22]. For sufficiently strong magnetic fields $eB \gg \Lambda_{\text{QCD}}^2$, it is reasonable to express the coupling constant α_s related to the magnetic field [13,25]. Motivated by the work of Miransky and Shovkovy [13], a similar ansatz for the magnetic-field-dependent coupling constant was introduced in the SU(2)NJL models [24]:

$$G(eB, T) = c(B)\left[1 - \frac{1}{1 + e^{\beta(B)[T_a(B)-T]}}\right] + s(B), \quad (21)$$

where the four parameters c, β, T_a, and s were obtained by fitting the lattice data and are strongly dependent on the magnetic field [24].

To identify the pseudocritical temperature of the cross-over transition, one generally uses the location of the peaks for the vacuum quark condensates $|\langle\bar{\psi}\psi\rangle|$ [18], or the normalized quark condensates [26,41],

$$\sigma = \frac{\langle\bar{\psi}\psi\rangle(B, T)}{\langle\bar{\psi}\psi\rangle(B, 0)}, \quad (22)$$

which means that the quark condensate is measured in units of the condensate at $T = 0$. In fact, the crossover is signaled by a rapid increase of the energy density. Thus, it has been suggested that the crossover transition is determined by the maximum of $-dM/dT$ [8], which is generally consistent with $d\phi/dT$ [42]. However, when the coupling constant runs with the temperature, a discrepancy will appear between them. From Eq. (2) we obtain the following relation:

$$\frac{dM}{dT} = -2G\frac{d\langle\bar{\psi}\psi\rangle}{dT} - 2\langle\bar{\psi}\psi\rangle\frac{dG}{dT}, \quad (23)$$

where the additional second term is necessarily introduced by the temperature dependence of the running coupling, and will lead to a new formula for the determination of the pseudocritical temperature in the next section.

III. NUMERICAL RESULTS AND DISCUSSION

For the SU(2) NJL model in this paper, we adopt the parameters $\Lambda = 650$ MeV, $m_u = m_d = 5.5$ MeV, and $G_0 = 4.50373$ GeV^{-2} in the calculation. In order to reflect the asymptotic freedom in the thermal region, the two kinds of running couplings are adopted for the zero magnetic field case and strong magnetic field case [1,24]. The temperature dependence of $G'(T)$ and the thermomagnetic dependence of $G(eB, T)$ were obtained by fitting lattice QCD predictions for the chiral transition order parameter.

A. In zero magnetic field

The quark condensate or the dynamical mass is usually considered as an order parameter of the chiral phase transition. The dynamical mass decreases as the temperature
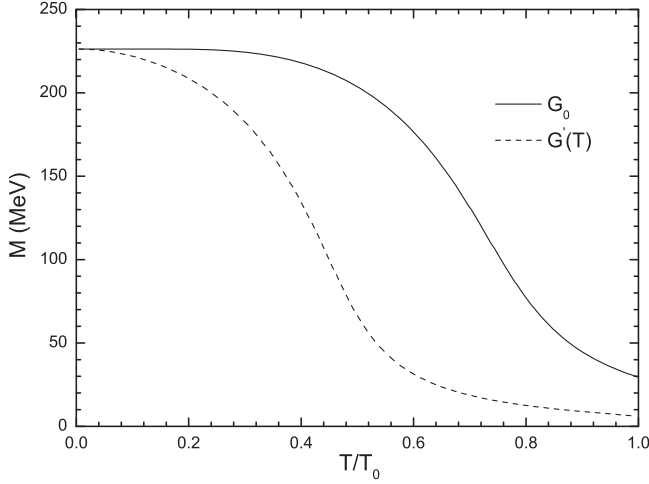
FIG. 1. The dynamical mass of the quark versus temperature for the coupling constant G_0 and the running coupling $G'(T)$. The critical temperature T_0 is 195 MeV.

FIG. 2. The entropy density divided by T^3 as a function of the temperature for the couplings G_0 and $G'(T)$.

increases, and the chiral-symmetric phase is restored. In this section, we mainly discuss the chiral restoration under the coupling constant G_0 and the temperature-dependent running coupling $G'(T)$ in zero magnetic field. The dynamical quark mass M is shown as a function of the temperature in Fig. 1. The solid and dashed lines are for the fixed coupling constant G_0 and the running coupling $G'(T)$, respectively. It is clear that the absolute value of the quark condensate under the running coupling $G'(T)$ is lower, which increases the possibility of having massless quarks compared to the fixed coupling constant G_0 case. Thus, the chiral-restoring transition can be realized at a lower temperature with the running coupling in our considerations.

According to the second law of thermodynamics, entropy is an increasing dimensionless function of temperature. In our work, we use the ratio of the entropy density and the cube of the temperature to get a dimensionless quantity in Fig. 2. The ratio increases and reaches a constant value ($S/T^3 = 9.2$) as the temperature increases. However, in the temperature range of 80–120 MeV, the dashed line for the running coupling $G'(T)$ is higher than the solid line for the fixed coupling G_0 case. The entropy density is increased by the running coupling $G'(T)$, which can be understood from the fact that the temperature-dependent interaction strength becomes weak enough as the temperature increases.

In Fig. 3, the sound velocity and specific heat are compared for the two different couplings, as in Fig. 2. The sound velocity reflects the stiffness of the equation of state, or determines the flow properties in heavy-ion reactions. In the left panel of Fig. 3, the sound velocity increases and gradually approaches the relativistic limit $c_s^2 = 1/3$ as the temperature increases. In the temperature range $0.4 \sim 0.8T_0$, we can see that the dashed line for the running coupling is always above the solid line for the fixed-coupling case. In fact, at high temperature, the quark
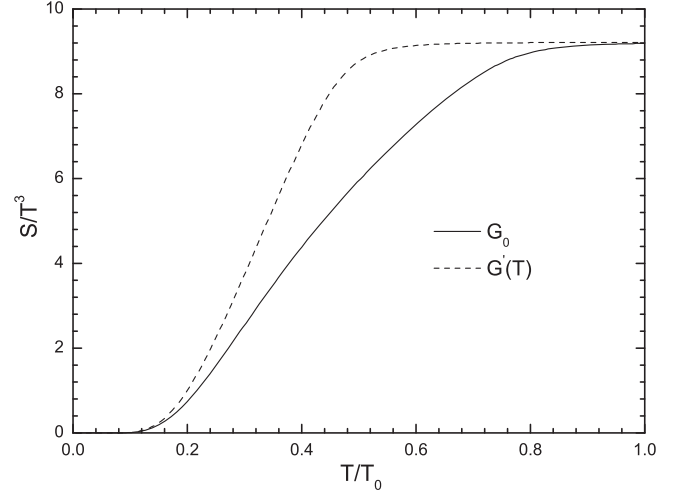
mass is much less in the running-coupling case than in the fixed-coupling case. The quarks with very small masses and weak interaction strengths display a behavior similar to the massless particles. So the running coupling induces a faster approach to the relativistic limit at lower temperature. In the right panel, the specific heat is shown as a function of temperature, where the ratio of the specific heat density C_V and the cubic temperature T^3 is introduced as a dimensionless quantity. The nonmonotonic shape of C_V/T^3 appears in both coupling cases. But for the running coupling, the position of the maximum of the specific heat moves in the direction of lower temperature, which would signifies that the crossover temperature may decrease in the running-coupling case compared to the fixed-coupling case. At very high temperature, the two lines coincide and the specific heat maintains an almost constant value of $C_V/T^3 \approx 28$, which indicates an equilibrium state of thermal radiation.
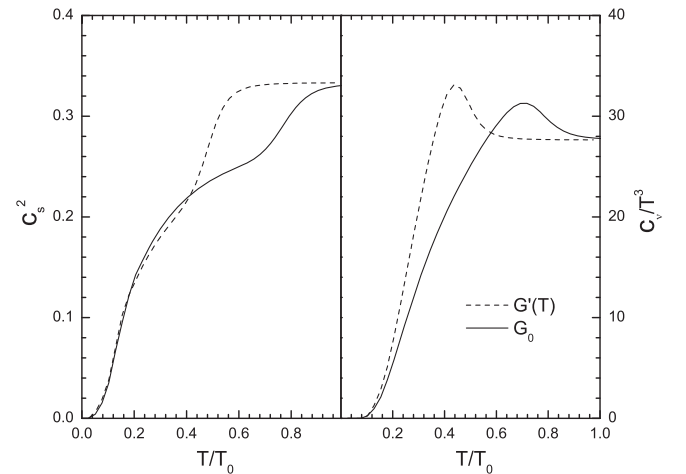

FIG. 3. Sound velocity and specific heat versus temperature. The two lines are coincident at T_0.
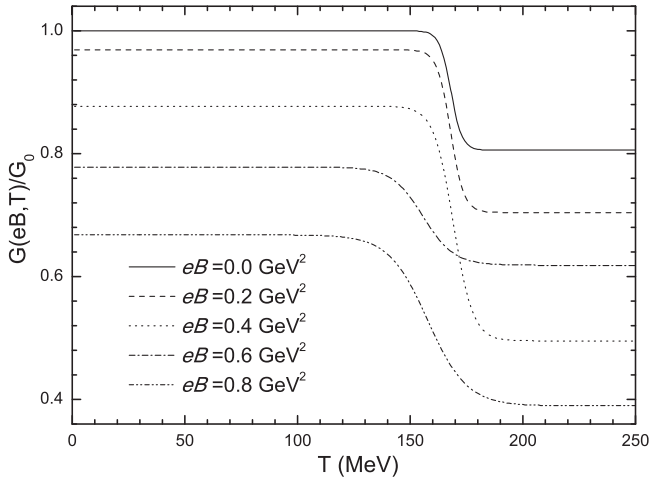
FIG. 4.   The reduced running coupling constant $G(eB, T)/G_0$ as a monotonous decreasing function of the temperature for several fixed magnetic fields.

B. In a strong magnetic field

It is well known that the dynamical quark mass and vacuum structure are drastically changed by a strong magnetic field and many interesting properties are revealed. In particular, the pseudocritical temperature for the chiral restoration transition characterized by inverse magnetic catalysis is a hot topic. Inverse magnetic catalysis can be interpreted by a magnetic-field-dependent coupling. In Fig. 4, we plot the reduced coupling $G(eB, T)/G_0$ versus the temperature at different magnetic fields $eB = 0$, 0.2, 0.4, 0.6, and 0.8 GeV^2. The coupling constant remains invariant when the temperature is smaller than 140 MeV. Moreover, the stronger the magnetic field, the smaller the coupling constant. Then, there is a sharp drop on each line at a critical temperature in the range of (150–170 MeV), which is essentially determined by the parameter T_a in the coupling constant (21). Due to the nonmonotonous parameter set of T_a in the coupling constant (21), the two lines for $B = 0.4$ and 0.6 GeV^2 cross each other. As in Ref. [24], the quark dynamical mass and the condensate decrease continuously when the temperature increases. So far, a large number of lattice simulations have demonstrated that there is only an energy density jump (and not a true phase transition) when the baryon chemical potential vanishes. This signals a crossover characterized by a pseudocritical temperature T_{pc}, which is about 160 MeV with systematic errors. The effect of the coupling constant running with the temperature was investigated and the entropy density can be greatly increased [24]. In this section, we focus on its effect on the crossover pseudocritical transition, which is determined by the peaks in the susceptibilities. In the following, we define two criteria to calculate the pseudocritical transition temperatures.

(1) Criterion I: The temperature T_{pc} at which the maximum of the derivation of the quark condensate ϕ with respect to the temperature occurs,

$$\frac{\partial^2 \phi}{\partial T^2} = 0. \qquad (24)$$

(2) Criterion II: The temperature T_{pc} at which the maximum of $-dM/dT$ occurs,

$$-\frac{d^2 M}{dT^2} = 2G\frac{\partial^2 \phi}{\partial T^2} + 2\phi\frac{\partial^2 G}{\partial T^2} + 4\frac{\partial G}{\partial T}\frac{\partial \phi}{\partial T} = 0. \quad (25)$$

Because the contribution of the last two terms in Eq. (25) cannot be neglected numerically, the two criteria in Eqs. (24) and (25) cannot be satisfied simultaneously. Even for the coupling constant $G(B, T) = G(B)(1 - \gamma T|eB|/\Lambda_{QCD}^3)$ [23], the second term is zero, but the third term will not vanish yet.

In Fig. 5 the derivation of the coupling constant $G(eB, T)$ with temperature is shown. In order to get a dimensional quantity, the quark condensate value in vacuum $|\langle \bar{\psi}\psi \rangle_0| = (236.4 \text{ MeV})^3$ is multiplied in the production. From the numerical result, it is obvious that the minimum value of the derivative $\partial G/\partial T$ occurs in the temperature range 140–175 MeV, which always covers the range of the pseudocritical temperature. Consequently, it is inevitable that the derivative term $\partial G/\partial T$ will affect the position of the crossover pseudocritical temperature T_{pc}. The parametrization of the temperature- and magnetic-field-dependent function from Ref. [23] will lead to a constant value for the second term in Eq. (23). Other attempts in the literature with a temperature-dependent
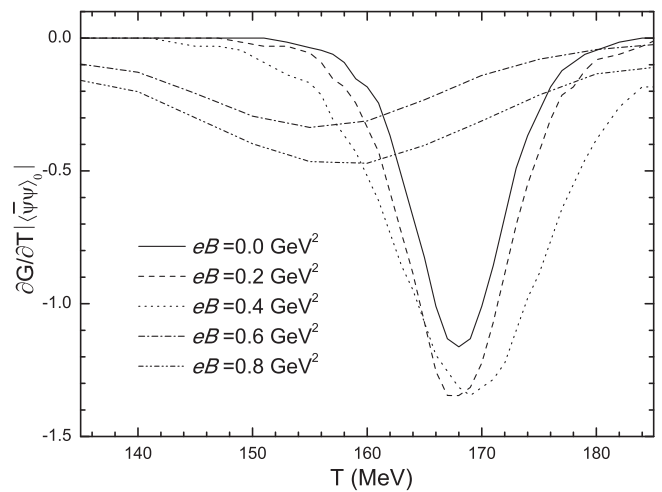

FIG. 5.   The derivative of the coupling constant with respect to the temperature, which is multiplied by the vacuum quark condensate $|\langle \bar{\psi}\psi \rangle_0|$ to give a dimensional quantity.
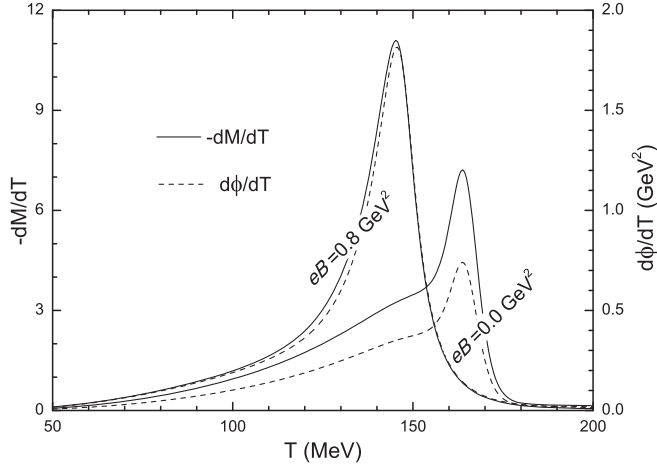
FIG. 6.   The pseudocritical temperature determined by the peaks of the derivatives $-dM/dT$ and $d\phi/dT$ is shown.

FIG. 7.   The pseudocritical temperature determined by the peaks of the derivatives $-dM/dT$ and $d\phi/dT$.

coupling have also led to considerable changes [43]. Because T_a is nonmonotonous in Eq. (21), the behavior of the curves as the magnetic field increases is not regular.

Since the behavior of the coupling with the temperature cannot be neglected, we compare the two criteria dM/dT and $d\phi/dT$ in the calculation of the pseudocritical temperature in Figs. 6 and 7. First, we show the contribution of the running coupling constant to the effective susceptibilities at the two strengths $eB = 0$ and $eB = 0.8$ GeV^2 in Fig. 6. For convenience of comparison, the negative derivative $-dM/dT$ (which is dimensionless) is plotted on the left axis, while the criterion $d\phi/dT$ (in units of GeV^2) is plotted on the right axis. The peaks of the susceptibility based on the two criteria are no longer exactly coincident, which is particularly noticeable for the magnetic field $eB = 0.8$ GeV^2.

Inverse magnetic catalysis can be explained by the dependence of the QCD coupling on the strong magnetic field. At finite temperature and vanishing density, it is further understood from the temperature- and magnetic-field-dependent coupling that the pseudocritical temperature decreases as the magnetic field increases. In order to account for the effect of $G(eB, T)$ and display the difference between the two criteria, we show the descending lines of the pseudocritical temperature T_{pc} as the magnetic field increases in Fig. 7. The solid and dashed lines are derived from the peaks of the derivatives $-dM/dT$ and $d\phi/dT$, respectively, in Fig. 6. For weak magnetic fields, the tiny difference can be neglected. As the magnetic field increases, the two lines are distinctly separated. It can be clearly seen at stronger magnetic fields that the criterion dM/dT will give a lower pseudocritical temperature T_{pc} and the inverse catalysis effect becomes more prominent. The parametrization of the running coupling is derived from the lattice
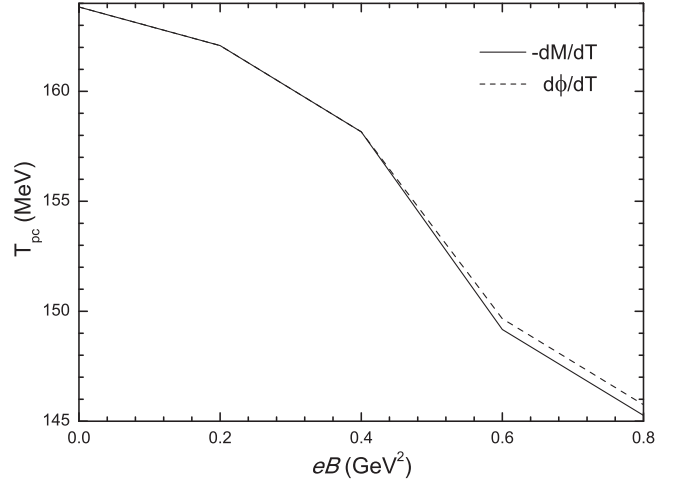
simulation of the QCD phase diagram, and in turn it will influence the QCD pseudocritical temperature. However, the difference between the two criteria is less than the lattice error. One cannot make a conclusion about which criterion is better to get the pseudocritical temperature. To some extent, the relation can be used to check the discrepancy between two methods for the running coupling proposed in future work.

IV. SUMMARY

In this paper we have employed the SU(2) NJL model to study QCD matter with a temperature- and/or magnetic-field-dependent coupling. Compared to the fixed coupling constant, the temperature-dependent coupling drastically changes the dynamical quark mass, entropy density, sound velocity, and specific heat. As the temperature increases up to T_0, the entropy density, sound velocity, and specific heat density go up and approach the critical values $S/T^3 \approx 9.2$, $c_s = \sqrt{1/3}$, and $C_V/T^3 \approx 28$. In the temperature range $0.4 \sim 0.8T_0$, we found that the entropy and sound velocity in the running-coupling case are remarkably larger than those in the fixed-coupling case.

It is also helpful to use the magnetic-field- and temperature-dependent coupling when accounting for inverse magnetic catalysis at finite temperature. In previous work, the position of the crossover transition characterized by a pseudocritical temperature was determined by the peak of the susceptibility of the quark condensate or the quark dynamical mass with respect to the temperature. The two criteria $d\phi/dT$ and dM/dT are coincident when the coupling is independent of the temperature. However, when the coupling constant depends on the temperature and magnetic field, a discrepancy will appear between the two criteria due to the presence of the nonzero term $\partial G(eB, T)/\partial T$.

The criterion dM/dT leads to a lower pseudocritical temperature for the crossover transition. The special value of T_{pc} will depend on the running behavior of the coupling constant with the temperature. Therefore, we argued that possible choices for the coupling constant in future work will influence the QCD phase diagram.

Up to now, spontaneous chiral symmetry breaking has been studied in backgrounds of electric and magnetic field [44]. The QCD phase diagram could be ruled by the rather complicated interaction structure. A careful treatment should be done in the case of the temperature- and magnetic-field-dependent coupling $G(eB, T)$. In a future paper, we hope to consider the implications for the color superconducting phase to develop a deeper understanding of the QCD phase diagram.

[1] V. Bernard, U.-G. Meissner, and I. Zahed, Phys. Rev. D **36**, 819 (1987).

[2] D. Lai, Rev. Mod. Phys. **73**, 629 (2001).

[3] V. A. Miransky and I. A. Shovkovy, Phys. Rep. **576**, 1 (2015); J. O. Andersen, W. R. Naylor, and A. Tranberg, Rev. Mod. Phys. **88**, 025001 (2016).

[4] G. H. Bordbar and A. R. Peivand, Res. Astron. Astrophys. **11**, 851 (2011).

[5] R. G. Felipe and A. P. Martínez, J. Phys. G **36**, 075202 (2009); R. G. Felipe, D. M. Paret, and A. P. Martínez, Eur. Phys. J. A **47**, 1 (2011).

[6] X. J. Wen, Phys. Rev. D **88**, 034031 (2013); X. J. Wen, S. Z. Su, D. H. Yang, and G. X. Peng, Phys. Rev. D **86**, 034006 (2012).

[7] D. P. Menezes, M. B. Pinto, and C. Providência, Phys. Rev. C **91**, 065205 (2015).

[8] G. N. Ferrari, A. F. Garcia, and M. B. Pinto, Phys. Rev. D **86**, 096005 (2012).

[9] U. Das and B. Mukhopadhyay, Phys. Rev. D **86**, 052001 (2012).

[10] D. Ebert, K. G. Klimenko, M. A. Vdovichenko, and A. S. Vshivtsev, Phys. Rev. D **61**, 025005 (1999).

[11] E. J. Ferrer and V. de la Incera, Phys. Lett. B **481**, 287 (2000); N. Mueller and J. M. Pawlowski, Phys. Rev. D **91**, 116010 (2015).

[12] V. P. Gusynin, V. A. Miransky, and I. A. Shovkovy, Phys. Rev. Lett. **73**, 3499 (1994); V. P. Gusynin, V. A. Miransky, and I. A. Shovkovy, Phys. Lett. B **349**, 477 (1995).

[13] V. A. Miransky and I. A. Shovkovy, Phys. Rev. D **66**, 045006 (2002).

[14] T. Inagaki, D. Kimura, and T. Murata, Prog. Theor. Phys. **111**, 371 (2004).

[15] D. P. Menezes, M. Benghi Pinto, S. S. Avancini, and C. Providência, Phys. Rev. C **80**, 065805 (2009); D. P. Menezes, M. B. Pinto, S. S. Avancini, A. P. Martínez, and C. Providência, Phys. Rev. C **79**, 035807 (2009); A. G. Grunfeld, D. P. Menezes, M. B. Pinto, and N. N. Scoccola, Phys. Rev. D **90**, 044024 (2014).

[16] P. G. Allen and N. N. Scoccola, Phys. Rev. D **88**, 094005 (2013).

[17] E. J. Ferrer, V. de la Incera, I. Portillo, and M. Quiroz, Phys. Rev. D **89**, 085034 (2014).

[18] R. Gatto and M. Ruggieri, Phys. Rev. D **82**, 054027 (2010).

[19] F. Preis, A. Rebhan, and A. Schmitt, J. High Energy Phys. 03 (2011) 033; F. Preis, A. Rebhan, and A. Schmitt, Lect. Notes Phys. **871**, 51 (2013).

[20] G. S. Bali, F. Bruckmann, G. Endrodi, Z. Fodor, S. D. Katz, S. Krieg, A. Schafer, and K. K. Szabo, J. High Energy Phys. 02 (2012) 044; G. S. Bali, F. Bruckmann, G. Endrodi, Z. Fodor, S. D. Katz, and A. Schafer, Phys. Rev. D **86**, 071502(R) (2012).

[21] V. P. Pagura, D. Gómez Dumm, S. Noguera, and N. N. Scoccola, Phys. Rev. D **95**, 034013 (2017).

[22] E. J. Ferrer, V. de la Incera, and X. J. Wen, Phys. Rev. D **91**, 054006 (2015).

[23] R. L. S. Farias, K. P. Gomes, G. Krein, and M. B. Pinto, Phys. Rev. C **90**, 025203 (2014).

[24] R. L. S. Farias, V. S. Timóteo, S. S. Avancini, M. B. Pinto, and G. Krein, Eur. Phys. J. A **53**, 101 (2017).

[25] M. Ferreira, P. Costa, O. Lourenco, T. Frederico, and C. Providência, Phys. Rev. D **89**, 116011 (2014).

[26] M. Ferreira, P. Costa, D. P. Menezes, C. Providência, and N. N. Scoccola, Phys. Rev. D **89**, 016002 (2014).

[27] V. M. Bannur, Phys. Rev. C **78**, 045206 (2008).

[28] K. Enqvist and K. Kainulainen, Z. Phys. C **53**, 87 (1992).

[29] J. C. Collins and M. J. Perry, Phys. Rev. Lett. **34**, 1353 (1975).

[30] C. F. Li, L. Yang, X. J. Wen, and G. X. Peng, Phys. Rev. D **93**, 054005 (2016).

[31] X. J. Wen and J. J. Liang, Phys. Rev. D **94**, 014005 (2016).

[32] L. Yang and X. J. Wen, Commun. Theor. Phys. **67**, 535 (2017).

[33] C. Ratti, Europhys. Lett. **61**, 314 (2003); M. Buballa and M. Oertel, Phys. Lett. B **457**, 261 (1999).

[34] T. Hatsuda and T. Kunihiro, Phys. Rep. **247**, 221 (1994).

[35] J. L. Richardson, Phys. Lett. B **82**, 272 (1979).

[36] M. Sinha, X. G. Huang, and A. Sedrakian, Phys. Rev. D **88**, 025008 (2013).

[37] J. F. Xu, G. X. Peng, F. Liu, D. F Hou, and L. W. Chen, Phys. Rev. D **92**, 025025 (2015).

[38] A. A. Natale, Nucl. Phys. B, Proc. Suppl. **199**, 178 (2010).

[39] S. S. Avancini, D. P. Menezes, and C. Providéncia, Phys. Rev. C **83**, 065805 (2011).

[40] T. Kojo and N. Su, Nucl. Phys. **A931**, 763 (2014).

[41] R. Gatto and M. Ruggieri, Phys. Rev. D **83**, 034016 (2011).

[42] S. S. Avancini, D. P. Menezes, M. B. Pinto, and C. Providência, Phys. Rev. D **85**, 091901 (2012).

[43] J. Roźynek and G. Wilk, J. Phys. G **36**, 125108 (2009).

[44] M. Ruggieri and G. X. Peng, Phys. Rev. D **93**, 094021 (2016).